25th ABCM International Congress of Mechanical Engineering
October 20-25, 2019, Uberlândia, MG, Brazil

COBEM2019-0743
CHARACTERIZATION OF THE FLAME DEVELOPMENT IN THE FIRST CYCLES OF OPERATION IN A SPARK IGNITION ENGINE FROM THE INJECTION MODES PFI AND DI FOR ETHANOL AND GASOLINE

Maycon Ferreira Silva
Pedro Teixeira Lacava
Technological Institute of Aeronautics, Laboratory of Combustion, Propulsion and Energy, São José dos Campos, SP, Brazil
mayconfsilva@yahoo.com.br, placava@ita.br

Abstract. *The characteristics of the first firing cycle were experimentally investigated for a single cylinder research engine PFI-SI and DI-SI with optical access, fueled with anhydrous ethanol and gasoline. Due to the fact the worse combustion during the initiation of an engine results in an increase of misfiring events and unstable combustion process, it is necessary to better understand the flame behavior and spatially propagation to improve the combustion especially in the start of the engine. High spatial resolution cycle resolved digital imaging, in the visible and UV spectral range was used to characterize the flame front propagation. A post-processing routine was developed to evaluate flame areas and global morphology characteristics to have a detail understanding of the flame behavior in the combustion chamber. The engine was fueled with ethanol (E100) and gasoline (G100). It was operated at 900 rev/min to study the behavior of the combustion process with low turbulent effects. The injection duration was set to a value of stoichiometric mixture when stable operation is reach. The results for the PFI suggest an increase in the flame area with the increase in the cycles of operation. In addition, a decrease in the flame deformation was measured. Absence of flame at the beginning of the process is also observed, followed by unstable combustion. For the DI mode, combustion reaches results close to the permanent thermal regime from the beginning, however with great cyclic variability.*

Keywords: *Combustion, First Cycles, SI Engines, Ethanol, Gasoline, Direct Injection, PFI.*

1. INTRODUCTION

In the last decades, for reasons ranging from energy security to environmental pollution regulations, much attention has been paid to the use of biofuels as alternative sources of energy in the transportation industry. Ethanol was identified as one of the most important renewable fuels for addressing these issues (Baeyens, J., et.al 2015 and Demirbas, et.al. 2016). In Brazil, ethanol has been considered as the main alternative to fossil fuels. Its strategic investments in ethanol influenced all sectors of the economy, including transportation, petroleum resource production and petroleum product manufacturing. In its anhydrous ethanol form (AEF), with a minimum alcohol content of 99.6% v/v, ethanol was used in the formulation of type C gasoline and was considered for gas stations in hydrated ethanol form (HEF) (Martinez, J. 2014).

Even if the use of ethanol as gasoline additive or replacement has been studied quite extensively, including the anhydrous and hydrated formulations and both in PFI and DI injection modes (Augoye, A., et.al. 2014 and Di Iorio, S., et.al. 2015). These studies are focused on the analysis of combustion and engine performance in warmed and steady running conditions. Few works are devoted to the investigation of the cold start regime in an SI engine fuelled with a high percentage of ethanol (Kumar & Kumar, 2017). On the other hand, one of the major drawbacks in applying highly concentrated ethanol in SI engines is cold start instability. This is due to the characteristics of ethanol, such as large latent heat required to vaporize.

To overcome these shortcomings, several solutions were tested. Fuel-rich injection during startup was applied to ensure ignition, but the over-supply of fuel and lean operation of the catalytic converter, produced large amounts of HC and CO emissions during the cold-start period. To boost vaporization and obtain high compression peak temperature, intake valve timing control was introduced, but the system requires changes in the engine system and control.

To minimize modifications in design and allow to fully exploit the benefits of ethanol fuelling, a deeper understanding of the combustion process in cold start conditions is necessary. To this aim, the paper investigates flame inception and propagation in an optically accessible SI engine fuelled with pure ethanol during startup compared to gasoline. Cycle resolved digital imaging allowed to follow the evolution of the first cycles of the combustion process since the spark ignition until the spreading of the flame in the combustion chamber. The development of custom image processing permitted to estimate the flame area and speed with high spatial and temporal resolution.

It is confirmed that the behavior of the first cycles of combustion is of great importance for all types of ignition engines, regardless of the mode of injection applied (Heywood, J. 1998 and Fan, L. 2013). Due to the heating period of the catalytic converter, high levels of UHC and CO are emitted during this period (Liu, S. 2017). Thus, control and knowledge of the combustion characteristics of the first cycles become an important field for the development of vehicle engines with the objective of greater efficiency and emission control.

2. EXPERIMENTAL PROCEDURE

To perform the experimental tests, an internal combustion ignition engine AVL 5406 with optical access, active AC dynamometer, injection line, acquisition system and control unit was used. The tests were performed by two types of fuel injection: PFI (Port Fuel Injection) and DI (Direct Injection). For a better understanding of the combustion process, thermodynamic and optical data were acquired.

The phenomenon used to obtain optical data was chemiluminescence, which is the conversion of chemical energy into visible light emission. Optical access to the combustion chamber is permitted by a fused silica window (72 mm diameter) attached to the piston ring. The radiation produced by combustion is reflected by a mirror suitable for the region of UV radiation inclined at 45°, fixed to the bottom of the elongated piston and then recorded by the acquisition system. Of the 82 mm piston diameter, the configuration was made in the 64 mm diameter field of view.

For this process, a high-speed PCO.Dimax S1 camera was used, coupled to a double intensifier VS4-1845HS. The detector was equipped with UV-Nikon 105mm f/4.5. The camera was adjusted to a rate of 5400 fps and 864x896 pixels of interest, corresponding to 1 image per crank angle at 900 rpm. For the level of intensification, the minimum gain value indicated by the manufacturer of 55,000 was maintained.

To investigate the transition of the first combustion cycles to a stable operating condition, the optical tests consisted of the acquisition of 62 frames per cycle after ignition, during the initial 80 consecutive engine cycles after the first injection. For all optical measurements, the synchronization between the cameras and the engine was done by the crank angle encoder signal.

Figure 1 illustrates the view obtained with the high-speed camera from the top of the cylinder, where the location of the exhaust and intake valves, spark plug, pressure transducer and the possible positions for the injector by direct injection can be observed. The spark plug is located 5 mm above the geometric center of the chamber.

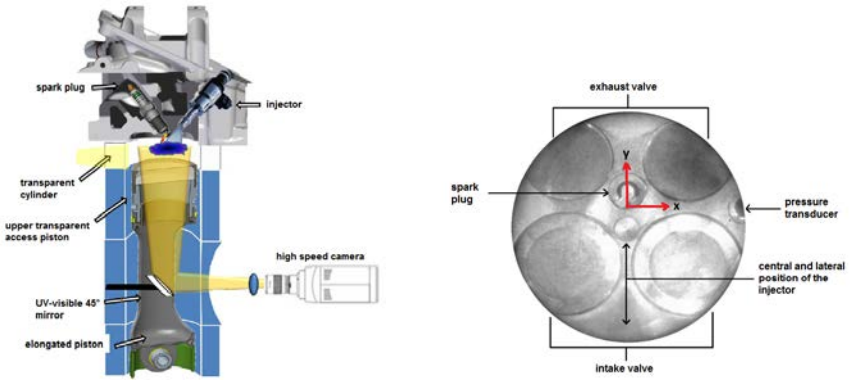

Figure 1. Schematic of the experimental engine apparatus with the high-speed camera (Adapted: Catapano et al., 2013) and combustion chamber geometry, with inlet and exhaust valves, spark plug and pressure transducer.

The engine speed was set at 900 rpm and throttle at 25% for the stoichiometric air-fuel ratio (λ). This parameter was adjusted for comparison of the first combustion cycles in a mode commonly used in regimen operation. The injection pressure used in the tests was 4.2 bar for the PFI and 150 bar for DI. To allow the formation of a homogeneous mixture during admission stroke, the injection was started at 290 °CA BTDC for the DI and 295°CA ATDC for the PFI mode injection. Concerning the moment of ignition, the optimum point of the operation was set to obtain the maximum torque of the engine (MBT), for the conditions stipulated for each fuel to optimize the combustion process (Tab. 1).

Table 1. Experimental setup for PFI and DI injections for λ = 1.0; throttle = 25% and rotation = 900rpm.

	PFI		**DI**	
	E100	G100	E100	G100
Injection duration	66 °CA	48 °CA	3,60 ms	2,60 ms
Ignition advance	06 °CA BTDC	00 °CA BTDC	12 °CA BTDC	04 °CA BTDC

For the studies carried out for behavioral analysis in the first combustion cycles, the fuels used were anhydrous ethanol (E100) and gasoline (G100). In Table 2, data on the characteristics of the fuels used are presented. Data on density, percentage and calorific value were obtained with the help of the IKA C1 calorimeter and DDM2911 digital densimeter.

Table 2. Properties of fuels.

Fuel	**E100**	**G100**
Molecular Formula	C_2H_5OH	C_8H_{18}
Density (20°C) [kg/m^3]	0,7901	0,7478
Water [%]	0,4	-
Anhydrous Ethanol [%]	99,6	-
HHV [kJ/kg]	29,112	43,452
Latent heat of vaporization [kJ/kg]*	918,7	341,9

(1) Latent heat values of vaporization obtained from AWAD et al. (2018).

To carry out the experimental tests, the room where the engine is located was conditioned to a temperature of 16°C. For each experimental test carried out, the operation of the engine without combustion (motorized) was initiated at a rotation of 900 rpm and the pre-selected load of 25% throttle. When this condition was reached, the high-speed camera was activated and then fuel injection, which in turn started the combustion process. A trigger system was used to synchronize the thermodynamic data with the recorded images. After completion of the cycles recorded by the high-speed camera, the injection process was interrupted and the engine switched off. The engine was kept in the operating room under a controlled external air temperature of 16°C and switched off for 15 minutes until a new operation occurred.

2.1 Image Processing

To obtain flame front propagation information such as size, shape, location and propagation characteristics, processing was developed in the Vision of National Instruments program.

To recover the geometric parameters of the flame, some steps were applied in the processing. As a first step, image processing extracted the intensity plane to obtain 8-bit gray level images (Fig 2a). Subsequently, an appropriate circular mask is introduced to correct reflections and lights around the optical access (Fig. 2b). After that, the threshold was applied to each image to obtain it binarized (Fig. 2c). To ensure that the entire image has the same percentage limit concerning the maximum, a normalization of the image was done by defining the maximum intensity pixel equal to the maximum of the 8-bit grayscale (255). After the threshold, the color inversion and morphological transformations were applied to fill the holes and remove small regions that are not part of the main flame, as observed in Fig. 2d. The flame contour was superimposed with the original image to verify the correct selection of the threshold value by direct visual comparison (Fig. 2e).

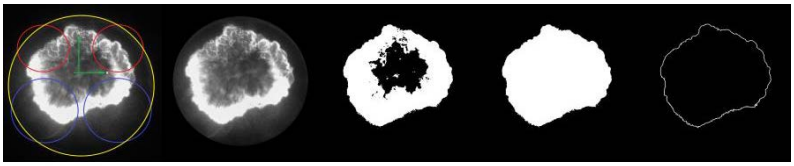

Figure 2. Image processing: (a) 8-bit original photographic record. (b) applied circular mask. (c) application of the threshold and binarization of the image. (d) gap filling. (e) Flame edge analyzed.

3. RESULTS

To better understand the effects of initial engine conditions on flame propagation, initially, image sequences were recorded for the first 30 cycles of operation. The recording period was from ignition to flame contact with the cylinder wall.

For the PFI mode, the combustion process presented well defined characteristics, indifferent to the fuels studied in this work. Images of the propagation of the first 30 combustion cycles are presented in Figs. 3-5. Figure 3 shows the first evidence of flame brightness after some cycles (5th cycle for E100 and 3rd cycle for G100). From this initial period, the propagation of the flame front was well detectable from the ignition to the optical limit. A marked increase in combustion luminosity is observed from the 11th cycle, in Fig. 4. Attaining cycle 21, the flame casing presents a higher regularity of development.

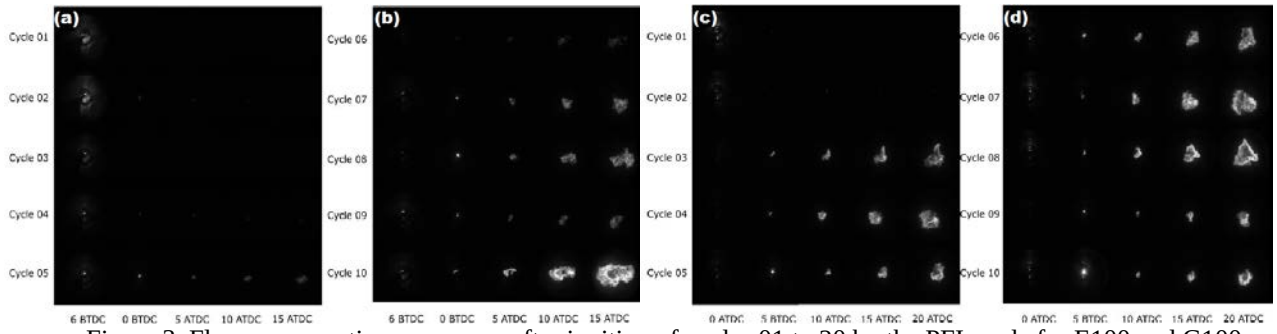

Figure 3. Flame propagation sequences after ignition of cycles 01 to 20 by the PFI mode for E100 and G100.

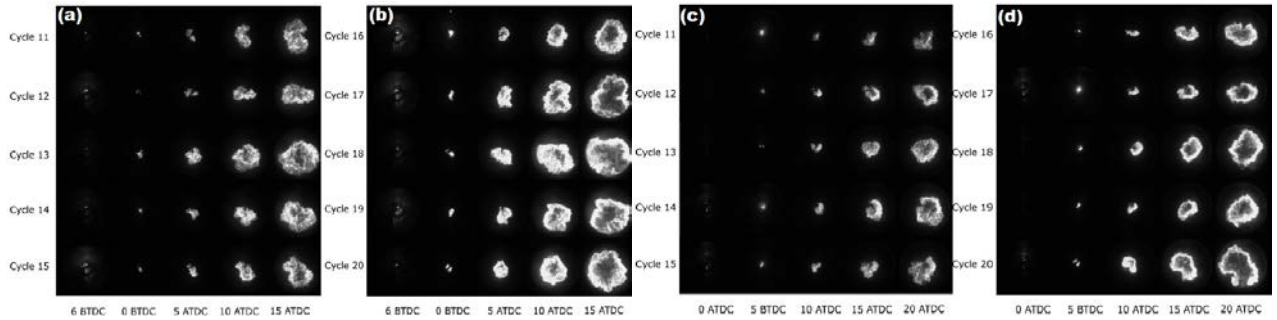

Figure 4. Flame propagation sequences after ignition of cycles 11 to 20 by the PFI mode for E100 and G100.

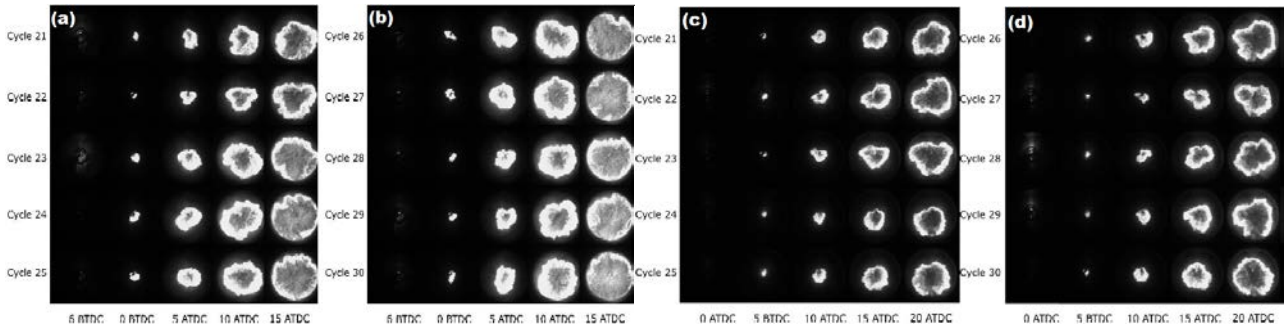

Figure 5. Flame propagation sequences after ignition of cycles 21 to 30 by the PFI mode for E100 and G100.

In addition to the images of the propagation of combustion by PFI mode, photographic records of the first 30 corresponding cycles for DI mode were also obtained (Figs. 6-8).

Differently from PFI mode, the DI mode already forms a flame nucleus in the first cycles, even in some cases without great intensity. Ignition failures and large variability in flame kernel behavior were common during this period. During direct injection operation, alternations between cycles are observed in a continuous variation of the behavior of the flame kernel, where there is a more expressive combustion in one cycle, followed by a faulty cycle and poorly developed flame.

Despite a certain cyclic variability in the intensity of combustion shown, there has always been ignition and propagation of the flame. Greater uniformity is presented in the development of the flame for both fuels with the progress of the cycles in the combustion process.

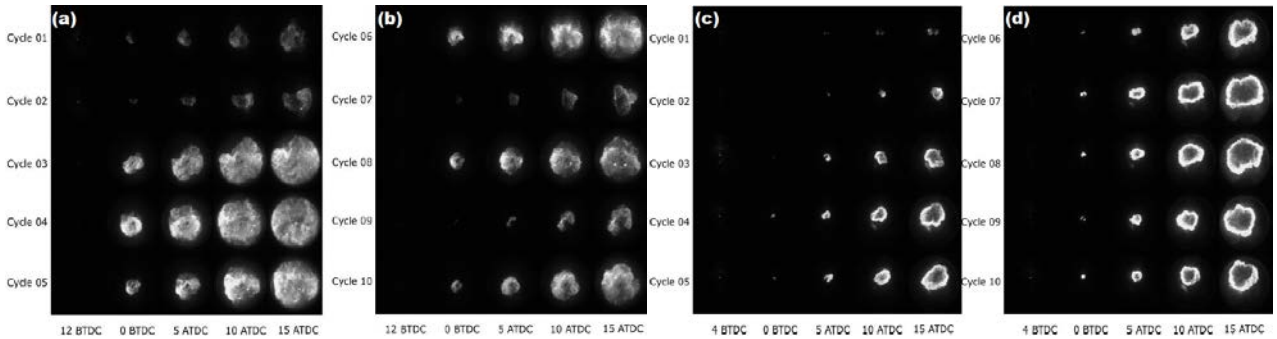

Figure 6. Flame propagation sequences after ignition of cycles 01 to 10 by the DI mode for E100 and G100.

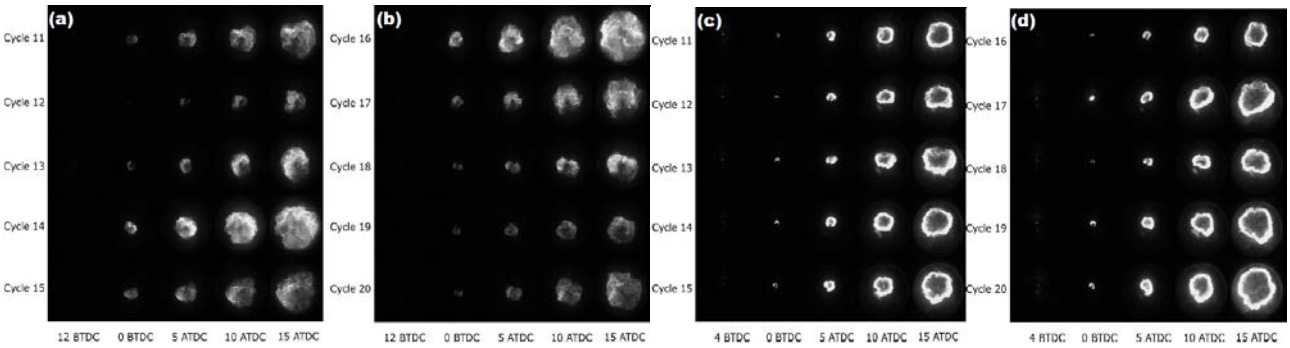

Figure 7. Flame propagation sequences after ignition of cycles 11 to 20 by the DI mode for E100 and G100.

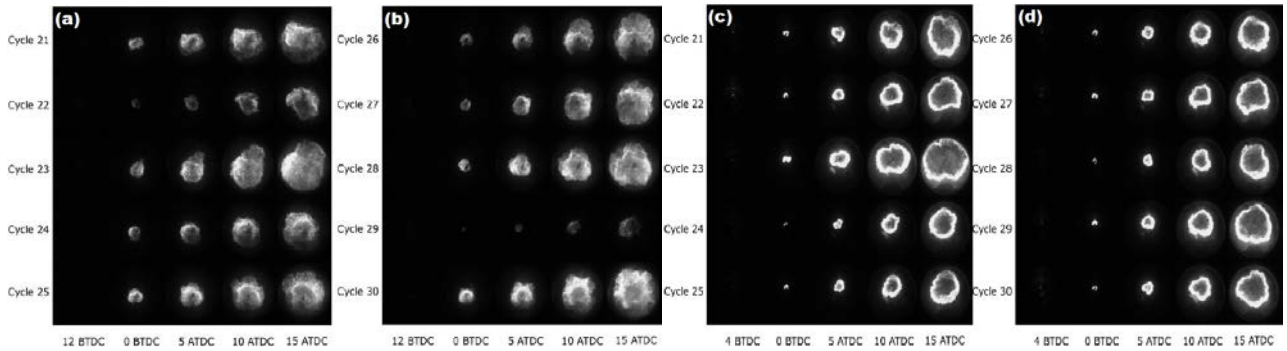

Figure 8. Flame propagation sequences after ignition of cycles 21 to 30 by the DI mode for E100 and G100.

With the images obtained with the high-speed camera and processing with the help of the Vision program, the evolution of the flame area for the first 30 combustion cycles was calculated, as shown in Fig 9. It is evident that as the operation progresses, the flame tends to develop better and with this, the flame velocity increases with time, which induces a significant change in the slope of the curves, approaching the end of the average curve of the engine in permanent thermal regime (RTP).

Among fuels, due to chemical characteristics, such as latent heat from vaporization, anhydrous ethanol (E100) presented difficulties in evaporation, especially in the first 15 cycles, with the absence and extinction of some burns, presenting less development of the flame area in this period in comparison with gasoline. On the other hand, G100, in spite of a slower burning at the beginning, it is possible to observe the propagation of the flame until the end of the process.

One of the possible reasons for the low development of gasoline, far from the permanent thermal regime, is the evolution of the burning and the value of the air-fuel ratio in the period studied. Despite the greater amount of volatile compounds and vaporization heat about three times lower than ethanol, vaporization difficulties were observed and forming a lean mixture, far from the stoichiometric ideal. The observed behavior may be linked to the theoretical energy supply to the engine per cycle that each fuel provides. With the same speed and air mass equal to the fuels, for the same λ, the adjustment of injected fuel quantity causes different theoretical energy release rates. Thus, with a higher air-fuel mass ratio, gasoline has less theoretical energy released than ethanol from this mode of operation used in these tests. This behavior reflects the low development of gasoline concerning ethanol for both injection modes.

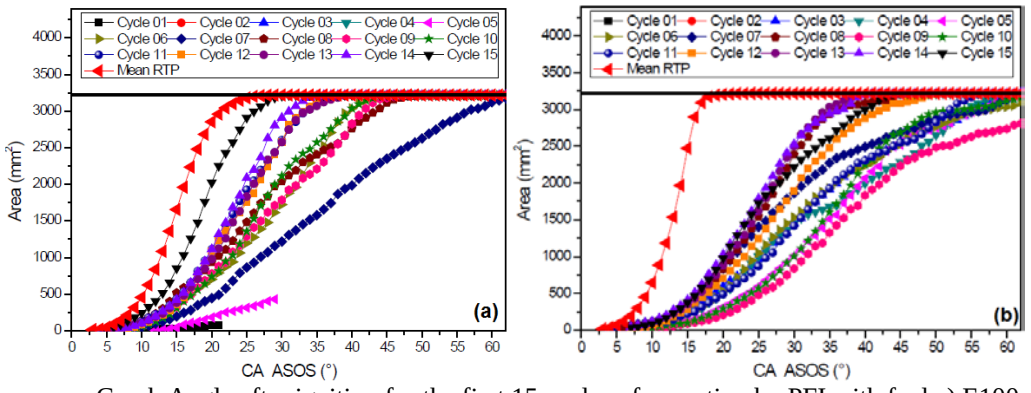

Figure 9. Area versus Crank Angle after ignition for the first 15 cycles of operation by PFI with fuel a) E100; b) G100.

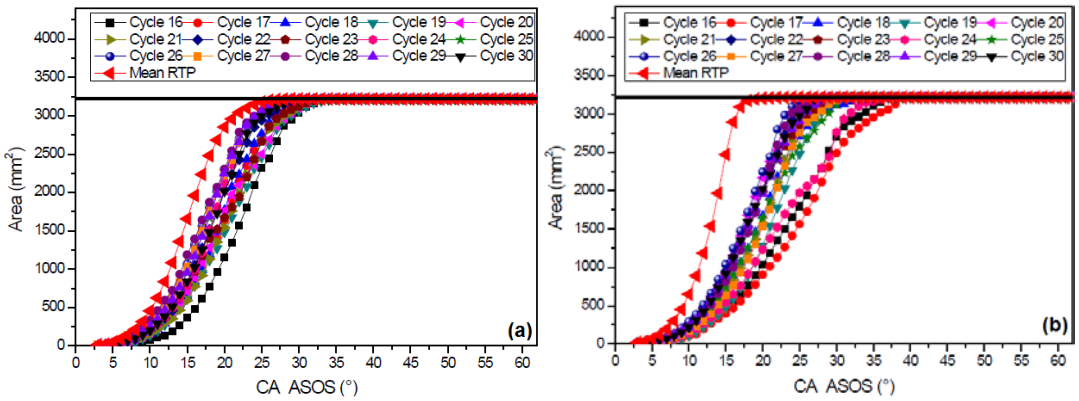

Figure 10. Area versus Crank Angle after ignition for 16 and 30 cycles of operation by PFI with fuel a) E100; b) G100.

Different from the data presented in the PFI mode, the injection through the DI mode (Fig. 11 and 12) already shows a development of the flame area close to the RTP, but with great variability. With higher injection pressure for DI mode, the vaporization of the fuel droplet allowed better fuel distribution and burning, even at lower temperatures in relation to the permanent thermal regime. As the process progresses, the temperature tends to stabilize, reaching a process with less cyclic variability.

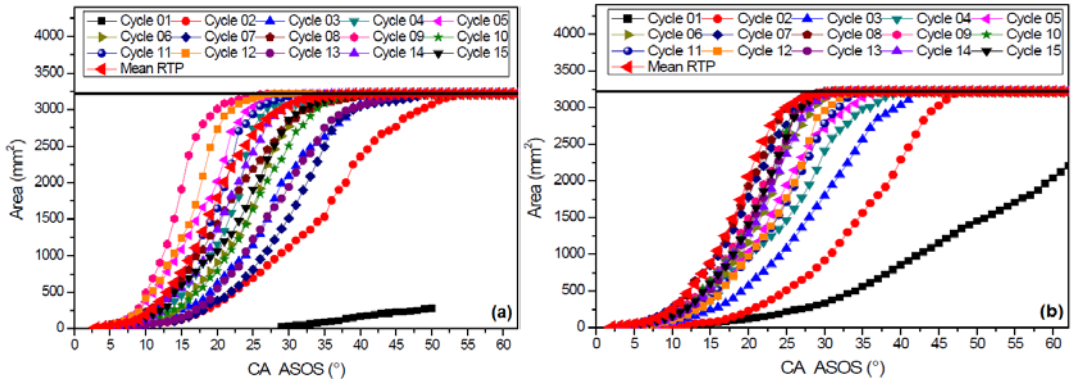

Figure 11. Area versus Crank Angle after ignition for the first 15 cycles of operation by DI with fuel a) E100; b) G100.

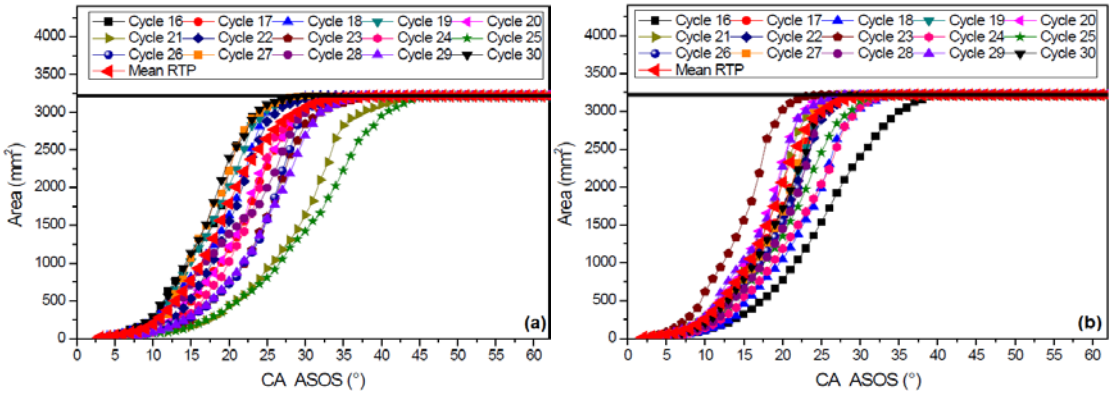

Figure 12. Area versus Crank Angle after ignition for 16 and 30 cycles of operation by DI with fuel a) E100; b) G100.

Fixing the crank angle in a developed period of flame evolution, the behavior of the first 80 combustion cycles was analyzed (Figs. 13 and 14). For the PFI, it is possible to observe an exponential behavior in the development of the flame growth process cycle by cycle. This behavior is repeated for both fuels, changing between them the slope of the curve. Thus, it is observed that the mode PFI has some stages of development. In the first stage, the low temperature in the combustion chamber and low evaporation in the intake manifold causes a very lean air-fuel ratio, inducing failures at the time of ignition. In the second stage, the air-fuel mixture is not yet in an adequate ratio due to incomplete evaporation of the fuel, however, there is already a condition of ignition and formation of an initial flame kernel. After that, in the third stage, there is a significant increase in the brightness of the flame corresponding to an improvement in evaporation and fuel distribution. At this stage, there is a considerable increase in the velocity of propagation and a decrease in flame distortion. Stage 4, is represented by a more stable condition both optical and thermodynamic, presenting only slight growth. For the fifth stage, the process reaches the permanent thermal regime, where a more

linear behavior with low cyclic variability is achieved. The duration of each stage is interfered by the characteristics of each fuel and its interactions.

For the DI mode, since the beginning of the combustion process, the evolution of the flame presents results close to the average, with high variability. In this case, ethanol is more affected by its chemical and physical characteristics. This high variability is also linked to possible fuel accumulations within the chamber that, due to low temperatures, may not vaporize. During these first combustion cycles, the fuel enters the cylinder and comes into contact with the combustion chamber at a low temperature. This condition causes heat loss from the fuel to the wall and engine parts, thus promoting less vaporization, and in some cases condensing the fuel. As a result, less fuel vapor and consequently less air-fuel mixture present at the time of combustion is generated, which causes incomplete combustion. In the next cycle, as the pressure temperature increases, the remaining fuel from the previous cycle evaporates and contributes to the combustion process (Hattori, 1997). As the operation progresses, the process tends to become more stable and the variability remains within the standard deviation.

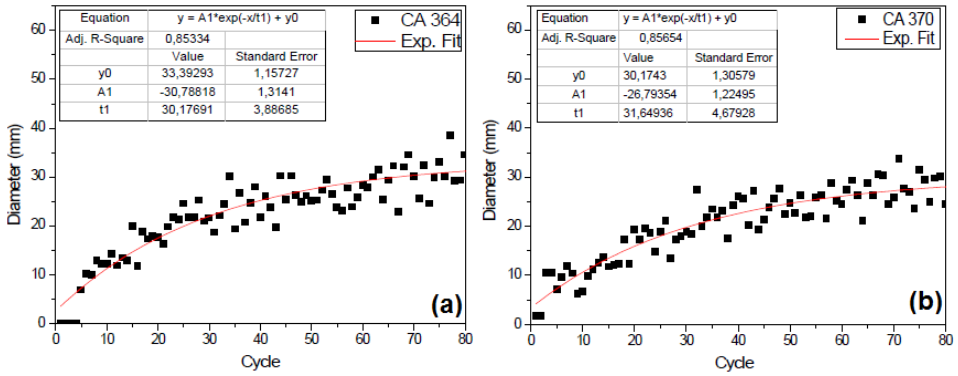

Figure 13. Diameter for the first 80 cycles of combustion versus cycles for fixed crank angle of 10 CA after ignition by PFI mode: a) E100; b) G100.

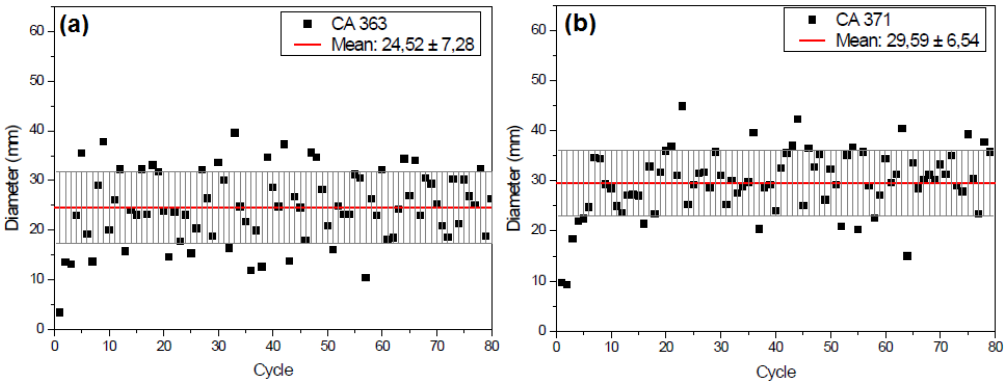

Figure 14. Diameter for the first 80 cycles of combustion versus cycles for fixed crank angle of 15 CA after ignition by DI mode: a) E100; b) G100.

For a global perspective of the combustion process, thermodynamic data were also analyzed. The pressure signals in the cylinder in relation to the crank angle of the first 80 combustion cycles were detected and analyzed, as shown in Figs. 15-18.

As presented in the optical data, the pressure signals of the first 15 consecutive cycles by the PFI mode show the effects of incomplete combustion. This effect is associated with temperature in the combustion chamber, the formation of the air-fuel mixture and inefficiency of vaporization for all fuels.

In the PFI mode, fuel was injected into the intake manifold while the intake valve was closed (exhaust period). Thus, with the valve and the entire intake manifold still at low temperature, the fuel has inefficient vaporization, which contributes to the formation of an inadequate mixture and consequently, ignition failures or improper combustion in these initial cycles.

After this period, with the valve and intake manifold already heated, the pressure development profile of the PFI mode for the two fuels is increasing, generating more expressive pressure results in the cylinder. Less variability is observed with the continuation of the combustion process.

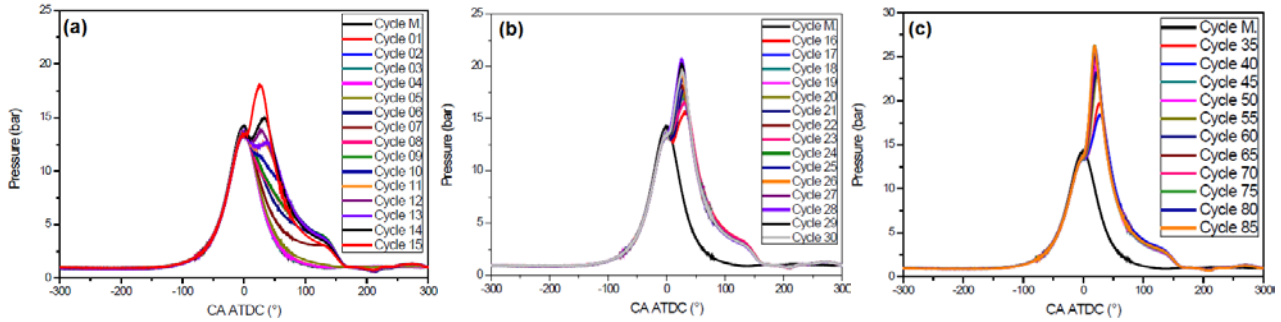

Figure 15. Pressure versus crank angle for the first 80 cycles of combustion by the PFI mode for E100.

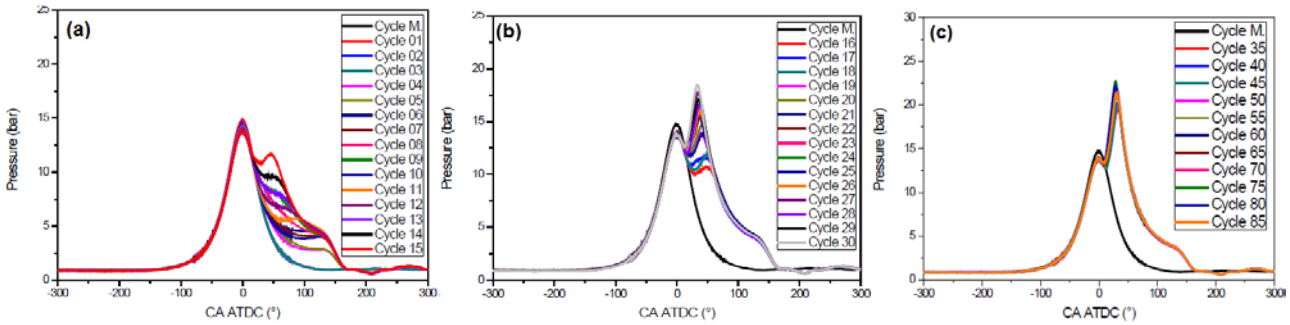

Figure 16. Pressure versus crank angle for the first 80 cycles of combustion by the PFI mode for G100.

The pressure curves also mirrored the operation of the motor between the optical and thermodynamic data for direct injection mode. Different from the pressure signals indicated by the PFI mode, the DI mode generated expressive cylinder pressure results from the start of the injection process. In this initial period, great variability is obtained and less chance of identifying in advance in which period will occur cycles with combustion failures. From the 16th cycle on, smaller variations and lower probability of absence of combustion concerning the first 15 cycles.

During the development of cycle pressure, one of the characteristics commonly observed is the alternating presence between cycles with higher pressure and cycles with much lower pressure. This profile, as discussed earlier, is due to unevaporated fuel from previous cycles that contribute to a richer mixture in the subsequent cycle, which provides higher cylinder pressure. This process releases the release of large amounts of hydrocarbon (HC) and carbon monoxide (CO) emissions due to incomplete combustion.

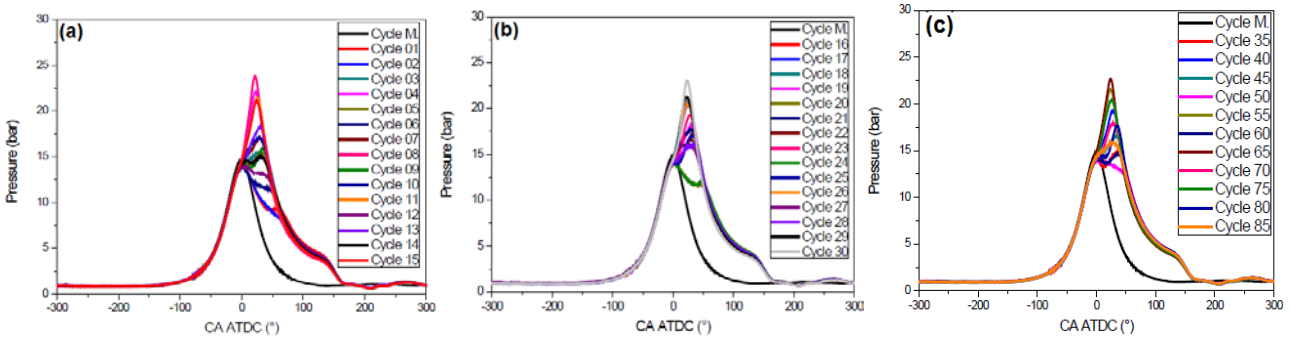

Figure 17. Pressure versus crank angle for the first 80 cycles of combustion by the DI mode for E100.

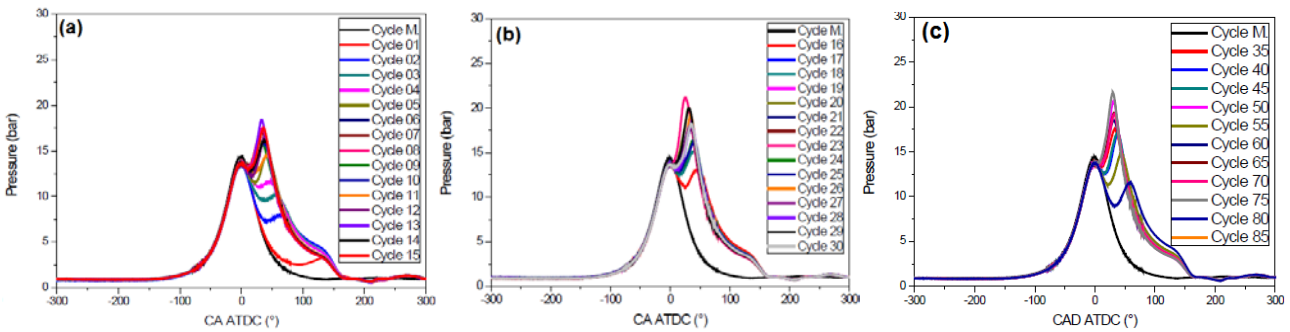

Figure 18. Pressure versus crank angle for the first 80 cycles of combustion by the DI mode for G100.

For the IMEP values presented in Fig. 19, negative values in the first cycles were presented for the two fuels, as a consequence of the failures recorded by the pressure transducer due to the absence of combustion or incomplete combustion. After this period, a rapid increase of the IMEP in a short period of cycles, where strong variability was measured in the fuels. Later, already close to the arithmetic mean, IMEP tends to increase with less variability and in a longer interval of time. Gasoline presented higher IMEP concerning anhydrous ethanol.

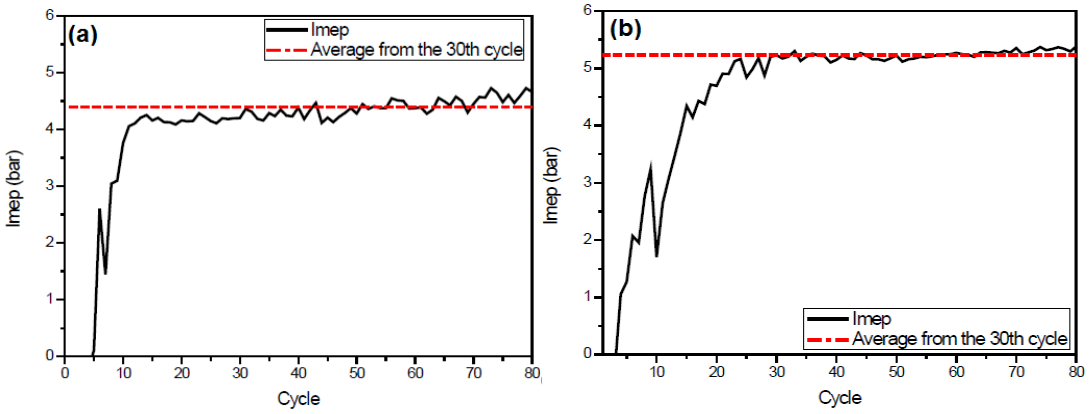

Figure 19. IMEP (bar) vs. cycles for first combustion cycles by PFI mode: (a) E100; (b) G100.

Table 2. Mean IMEP, maximum and coefficient of variation for fuels evaluated by PFI mode from cycle 30.

	E100	**G100**
IMEP mean [bar]	4,39	5,24
IMEP max [bar]	4,87	5,38
CovIMEP [%]	3,5	1,3

Despite the combustion failures that occurred in the first cycles, which caused low IMEP's, the values for the studied period present low standard deviation. Behavior and values match the thermodynamic data already presented. Due to the physical-chemical characteristics of gasoline, low cyclic variability was provided concerning ethanol.

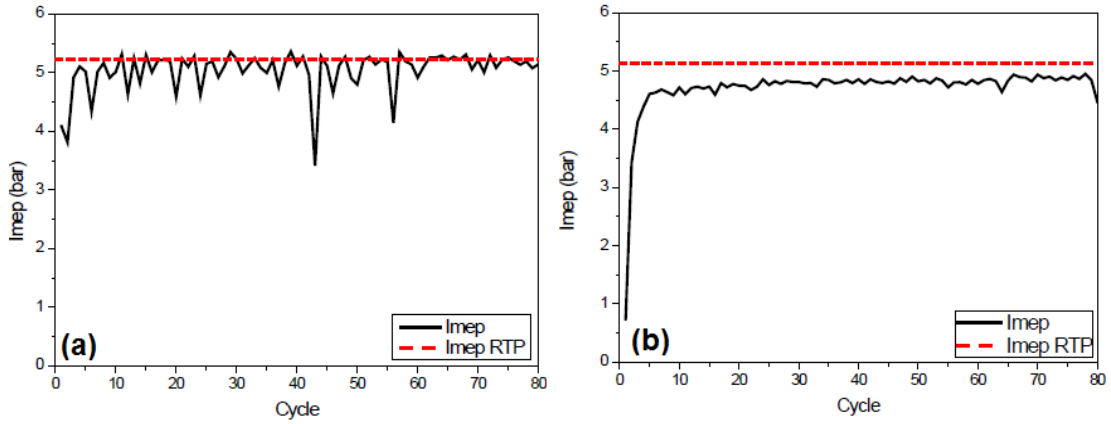

Figure 20. IMEP (bar) versus cycles for the first DI combustion cycles: (a) E100; (b) G100.

Table 3. Mean IMEP, minimum and coefficient of variation for the fuels evaluated by lateral DI mode.

	E100	**G100**
IMEP mean [bar]	5,04	4,71
IMEP max [bar]	5,36	4,95
CovIMEP [%]	6,7	10,4

4. CONCLUSION

In the present work, the optical and thermodynamic data of the first combustion cycles for PFI and DI with E100 and G100 fuels were analyzed. The results show a high sensitivity of the optical diagnosis and consistent with the thermodynamic data. This demonstrates that optical data and flame morphology studies are a powerful tool for investigations of combustion processes.

The adverse operating conditions of the first combustion cycles, such as low temperature in the internal parts of the cylinder and the intake manifold, manifest difficulties in fuel evaporation and inefficient formation of the air-fuel mixture. From this point on, incomplete combustion, ignition failures and absence of flames are observed with a certain frequency in this period. One of the factors that influenced the failures provided in this period of operation is the physical-chemical characteristics of each fuel. Difficulties are observed for both ethanol and gasoline during the initial cycles. Due to the high latent heat of ethanol and the low temperature inside the combustion chamber, the fuel presents evaporation difficulties. As the temperature increases, this effect is minimized and the combustion process approaches the permanent thermal regime (RTP).

Among the injection modes, the PFI presented an exponential growth profile of the flame front until reaching the stable period, with difficulty of flame formation at the beginning of the process. For this injection mode, five steps were identified in the initial combustion process studied. In the first step, combustion failures and absence of flames are induced due to inefficient vaporization caused by low temperature in the intake manifold, in the intake valve (closed at the moment of injection) and in the combustion chamber. In a second stage, the beginning of the flames presents itself with low development and release of energy due to the mixture of air and fuel not yet adequate, λ very lean. In the third stage, it is observed that the flames provide better vaporization and consequently higher brightness of the flame. The fourth stage is characterized by a more stable condition of flame propagation and less variability of morphological parameters. Finally, in the last stage, the combustion reaches a period of stability.

On the other hand, the direct injection mode (DI), different from the PFI, presented expressive results since the beginning of the process, with values always close to the mean values. For both fuels, despite the rapid thermodynamic response from the beginning, sporadic failures are displayed as incomplete combustion and combustion failures, which causes high process variability. With the progress of the combustion process, the variability tends to decrease and enter into a permanent thermal regime condition.

5. ACKNOWLEDGEMENTS

This work was supported by FAPESP-PSA.

6. REFERENCES

Augoye, A. and Aleiferis, P., 2014. “Characterization of Flame Development with Hydrous and Anhydrous Ethanol Fuels in a Spark-Ignition Engine with Direct Injection and Port Injection Systems”. *SAE Technical Paper* 2014-01-2623, doi:10.4271/2014-01-2623.

Baeyens, J., Kang, Q., Appels, L., Dewil, R., Lv, Y., & Tan, T., 2015. “Challenges and opportunities in improving the production of bio-ethanol”. *Progress in Energy and Combustion Science*, 47, 60-88.

Catapano, F., Sementa, P., Vaglieco, B. M., 2013. “Optical characterization of bio-ethanol injection and combustion in a small DISI engine for two wheels vehicles. *Fuel*, v. 106, p. 651–666.

Demirbas, A., & Demirbas, B., 2016. “Sustainable rural bioenergy production for developing countries”. *Energy Sources*, Part A: Recovery, Utilization, and Environmental Effects, 38(24), 3578-3585.

Di Iorio, S., Sementa, P., and Vaglieco, B., 2015. “Experimental Characterization of an Ethanol DI - Gasoline PFI and Gasoline DI - Gasoline PFI Dual Fuel Small Displacement SI Engine". *SAE Technical Paper* 2015-01-0848, doi:10.4271/2015-01-0848.

Fan, Q., Li, L., 2013. “Study on first-cycle combustion and emissions during cold start in a TSDI gasoline engine”. *Fuel*, 103: 473-479.

Heywood, J. B., 1988. “*Internal Combustion Engine Fundamentals”*. McGraw-Hill.

Kumar G, S. and Kumar, G., 2017. “Initial Development of a E85 Fueled, Multi Cylinder, Turbocharged, Spark Ignited, Heavy Duty Engine” *SAE Int. J. Engines* 10(1):55-60, doi:10.4271/2017-26-0075.

Liu, S., Clemente, E. R. C., Hu, T., & Wei, Y., 2007. “Study of spark ignition engine fueled with methanol/gasoline fuel blends”. *Applied Thermal Engineering*, 27(11), 1904-1910.

Martinez, J., 2014. “Measuring the Effects of Ethanol and Flex-Fuel Vehicles on Brazilian Gasoline Supply and Demand: A Simultaneous Equations Approach. In Energy & the Economy”, *37th IAEE International Conference*, June 15-18, 2014. International Association for Energy Economics.

Hattori, F. Analysis of fuel and combustion behavior during cold starting of SI gasoline engine. *JSAE Review*, v. 18, n. 4, p. 351–359, 1997.

7. RESPONSIBILITY NOTICE

The authors are only responsible for the printed material included in this paper.